Removing High Density Impulse Noise via a Novel Two Phase Method Using Fuzzy Cellular Automata

Mohammad Mehdi Piroozmandan [1], Fardad Farokhi [*2], Kaveh Kangarloo [3], Mohsen Jahanshahi [4]

[1,4] Department of Computer Engineering, Central Tehran Branch, Islamic Azad University, Tehran, Iran,
moh.piroozmandan.eng@iauctb.ac.ir, mjahanshahi@iauctb.ac.ir
[2] Department of Biomedical Engineering, Central Tehran Branch, Islamic Azad University, Tehran, Iran, f_farokhi@iauctb.ac.ir
[3] Department of Electrical Engineering, Central Tehran Branch, Islamic Azad University, Tehran, Iran, K_kangarloo@ iauctb.ac.ir

Abstract

In this paper, a novel method named RHDINTPM (Removing High Density Impulse Noise via a Novel Two Phase Method) is proposed for de-noising digital images corrupted by impulse noise. The proposed method is based on cellular automata (CA) and fuzzy cellular automata (FCA). In this method, a given image is mapped to a CA. That is, every pixel of the image is associated with a cell of CA. RHDINTPM is composed of a two-phase filter. The first phase of the proposed method is a two-step noise detector so in the first step the corrupted pixels are diagnosed by the intensity of the minimum value and average Moore neighborhood pixels for central Pixel. In the second step, in order to increase accuracy in improving noise detection, the uncorrupted pixels remained from the first step are investigated by cellular automata. In the second phase of the method, the defective pixels of two-dimensional fuzzy cellular automata are restored using the structure of the Moore neighborhood. The experimental analysis demonstrates that the proposed filter is robust enough to very high levels of noise as high as 90% and preserves the meaningful detail of the image. In addition, the proposed approach outperforms other representative filtering techniques in terms of image noise suppression and detail preservation.

Keywords: cellular automata, fuzzy cellular automata, noise detection, de-noising.
Article history: Received 27-July-2021; Revised 13-Aug-2021; Accepted 18-Aug-2021.

1. Introduction

Images are often corrupted by impulse noise (IN) and how to efficiently remove this kind of noise is an important research task. Impulse noise in a digital image may occur because of bit errors in transmission or maybe they are result of errors in the image during the acquisition process. Additionally, impulse noise maybe caused by errors during the data capture from digital cameras, faulty memory in hardware, and result of errors in data transmission generated in noisy sensors or noisy communication channels, and atmospheric turbulence [1-3].

Random-valued noise and salt and pepper noise are two common types of impulse noises that can degrade the image quality and cause great loss of important details in the image. For images corrupted by random-valued noise, noisy pixels can take any random value between the minimum and maximum values in the dynamic range. For images corrupted by salt and pepper noise, noisy pixels can take only two values the highest and the lowest value in the dynamic range. So, the effective removal of noise from an image is an important issue and facilitates the performances of subsequent image processing operations, such as edge detection, object recognition, image segmentation and compression [1-3]. There are many techniques and methods on the restoration of images corrupted by impulse noise [4-6, 40-46]. Mean filter and least mean square (LMS) adaptive filter [3] are linear filtering techniques that are not effective in removing impulse noise from an image. Linear filtering techniques can damage the uncorrupted pixels and can tend to blur sharp edges and also destroy lines and other fine image details. Also, non-linear filtering techniques can be used for the restoration of images corrupted by impulse noise. The median filter is well-known and is one of the most popular nonlinear filters. For removing impulse noise from

an image, the median filter is an effective noise removal method, which is computationally efficient [7]. When the noise density is higher (over 50%), the median filter smears some of the details and edges of the original image [8]. Many techniques are based on median filter which are nonlinear filters such as:

- Adaptive Median Filter (AMF) [9] which used variable window size for corrupted pixels removal
- Center-Weighted Median Filter (CWMF) [10] which is a filtering technique that gives more weight only to the central value of a window,
- Adaptive Center Weighted Median (ACWM) filter [36] and Recursive Weighted Median Filter (RWMF) [11],
- Tri-State Median Filter (TSMF) [12] incorporates the standard median (SM) filter
- Center-Weighted Median (CWM) filter to determine noise pixel.

These filters are modified and improved by the performance of the median filter. Applying these filters would inevitably remove image details contributed from the uncorrupted pixels, destroy image quality and intensities and cause additional blurring. Recently, some techniques using the fuzzy systems and artificial neural networks are used for de-noising and specifications of impulse noise on different points of the image that have done an effective role in image noise detection and reduction. In [13], a novel adaptive iterative fuzzy filter for de-noising images corrupted by impulse noise is proposed that consists of two stages detection of noisy pixels with is an adaptive fuzzy detector. In [14], a novel filter called CM filter is presented that is novel adaptive detail-preserving filter based on the cloud model (CM) to remove impulse noise. In [15], a new fuzzy method is proposed for filtering color images corrupted with additive impulse noise, and an impulse noise detector is used initially to detect the impulse noise which is presented in the filter. A novel method for the removal of impulse noise is called CAFSM which is proposed in [16] that is composed of a cascaded easily to implement impulse detector and a detail preserving noise filter. Also, other different techniques such as fuzzy-based two-step filter [17], fuzzy wavelet shrinkage and fuzzy logic controller have been proposed for restoring images corrupted with additive impulse noises [18-19]. To detect the noise even at a high level, good filter have been used, but due to its major role and its effects in image details, two problems were identified. One problem was that the edges were not recovered clearly and secondly, there was a lack of complexity, especially at the highest noise level.

In this paper, a novel method is proposed for repairing images damaged by impact noise. The proposed method consists of a two-phase filter based on cellular automata and fuzzy cellular automata. In the first phase, the proposed two-step method is used to identify and detect corrupted pixels. In the first step of the first phase, the standard deviation ratio is used between the maximum value and the mean value of the central cell neighborhood, which is considered a determinant of the cellular automata transfers function and the central pixel status. In the second step of the first phase, to improve the accuracy of the corrupted pixels detection, the pixels that were previously identified as uncorrupted pixels are re-identified and checked for noises. To do this, a Gaussian membership function is used to identify and detect corrupted pixels. The second phase of the proposed method uses two-dimensional fuzzy cellular automata with neighborhood Moore structure to repair the defective pixels and the noisy pixels that are detected in the first phase. The advantage of the Gaussian membership function is the smoothness and non-zero values at all points. The efficiency of the proposed method is tested using standard images and compared with the other algorithms.

2. Cellular automata and fuzzy cellular automata

Ulam and Von Neumann [17, 18] described the cellular automaton (CA) and Stephen Wolfram developed the CA theory [19], which can be used as a model for investigating the behavior of complex systems. CA is discrete dynamic system, which its behavior is completely based on local relations and the collection of a regular spatial lattice of cells, which each can have a finite number of states. The time is discrete in CA and the state of a cell is a function of the previous states of its neighbor cells. Also, CA is an effective tool for image processing [20] based on its simplicity and parallelism. The cell states are updated in discrete time steps and defined by its original state and surrounding neighborhood of cells with the help of a specified transition local and uniform rule. The simplest form of CA is one-dimensional CA and other models of CA can be defined such as two dimensional and three-dimensional ones. Cellular Automata can be defined by four tuple {L, Q, r, f}, where "L" is the regular grid of cells, "Q" a finite set of states, "r" and "f" are neighborhood radius and transition function. In a 3-neighborhood dependency, the next state $Q_i(t+1)$ of a cell is assumed to be dependent only on itself and on its two neighbors (left and right) as equation (1).

$$Q_i(t+1) = F(Q_{i-1}(t), Q_i(t), Q_{i+1}(t)) \quad (1)$$

Where F is transition function and referred to as the rule of the automata which depends on the

current states of the neighbors, Q_i demonstrates the state of the i^{th} cell at t^{th} instant of time. Any i^{th} cell, CA is configured with the rule R_i (rule vector $R = (R_1 \dots R_n)$, i=1…n) which 2^{2^3} distinct rules are in a 2-state 3-neighborhood CA. Types of different neighborhood structures are used for cellular automata, Von Neumann and Moore neighborhood structures are most commonly used (see fig.1). The generalized Von Neumann and Moore neighborhood of radius *r*=1 and r=2 has equation (2) and (3).

$$x_{(i,j)} = \{(i',j')\epsilon L \mid |i'-i| + |j'-j| \le 1\} \quad , \\ x_{(i,j)} = \{(i',j')\epsilon L \mid |i'-i| \wedge |j'-j| \le 1\} \tag{2}$$

$$x_{(i,j)} = \{(i',j')\epsilon L \mid |i'-i| + |j'-j| \le 1\} \quad , \\ x_{(i,j)} = \{(i',j')\epsilon L \mid |i'-i| \wedge |j'-j| \le 1\} \tag{3}$$

Where, L is a regular lattice (the elements of L being called cells) and N is a finite set of neighborhood indices such that ∀r∈L. In CA, the local rules are all crisp, but the descriptions of many actual models are uncertain and difficult to calculate by using crisp data. So, FCA (Fuzzy cellular automata) which is a particular type of continuous cellular automata where the local transition rule is fuzzy which takes the current membership value of each neighbor and calculates the value of membership of the next state, where used. FCA was introduced in [21] and some of their properties have been studied in [22, 23]. CA is used as a method for noise removal in the corrupted image and improving image quality in [24]. CA and fuzzy logic theory in [25] was proposed to restore digital images corrupted by impulse noise which this method describes a local fuzzy transition rule which gives a membership value to the corrupted pixel neighborhood and assigns next state as the central pixel value. In [26] a hybrid method based on cellular automata (CA) and fuzzy logic were used as a filtering tool for impulse noise reduction from images. This research shows that FCA can be used as an efficient tool for image processing purposes such as the restoration of images corrupted by impulse noises.

3. Method

In the proposed method, a novel impulse noise reduction from images is proposed. The proposed noise detector, which is the main contribution of this paper, consists of two steps. The corrupted pixels identified by the double noise detector were restored using fuzzy cellular automata based on their neighbor uncorrupted pixels. The flow chart of the proposed method is shown in Fig (4).

A) First phase

In this phase, a window of size 3*3 is used and $C_{i,j}$ is centered at (i,j) coordination (see fig.2). The goal of the first phase is detecting corrupted pixel in a selected window. Each corrupted pixel in image is corrupted by impulse noise has a significant change compared with its neighbors.

In the first phase, the double noise detector consists of two steps. At first, noise candidates are identified with the two dimensional cellular automata with Moore neighborhood (see fig.2). The state of cell at time $t+1$ depends on the states of itself and the neighborhood cells at time "t". It is based on transition function F and the cell states are updated in discrete time steps based on transition function F. $C_{i,j}^{t+1}$is the next state of cell in (i,j) coordination that can define $(t+1)^{th}$ state and transition function based on time and neighborhood pixels for Moore neighborhood as equation (4). Eq.(4) shows $C_{i,j}^{t+1}$ which is the next state of cell in (i,j) coordination with states that are updated in discrete time steps based on transition function F.

$$\mathrm{C}_{(\mathrm{i,j})}^{(\mathrm{t+1})} = \mathrm{F}\begin{pmatrix} \mathrm{C}_{(\mathrm{i+1,j})}^{(\mathrm{t})}, \mathrm{C}_{(\mathrm{i+1,j-1})}^{(\mathrm{t})}, \mathrm{C}_{(\mathrm{i,j-1})}^{(\mathrm{t})}, \mathrm{C}_{(\mathrm{i-1,j-1})}^{(\mathrm{t})}, \\ \mathrm{C}_{(\mathrm{i-1,j})}^{(\mathrm{t})}, \mathrm{C}_{(\mathrm{i-1,j+1})}^{(\mathrm{t})}, \mathrm{C}_{(\mathrm{i,j+1})}^{\mathrm{t}}, \mathrm{C}_{(\mathrm{i+1,j+1})}^{(\mathrm{t})} \end{pmatrix} \tag{4}$$

Where, $C_{(i,j)}^{(t+1)}$ is the next state of cell in (i,j) coordination. In the first step, standard deviation between the maximum and average of neighborhood cells in the CA is calculated using equations (5).

$$C_{average}^{d} = \frac{1}{N}\sum \begin{pmatrix} C_{i-1,j-1}, C_{i-1,j}, C_{i-1,j+1}, C_{i,j-1} \\ C_{i,j+1}, C_{i+1,j-1}, C_{i+1,j}, C_{i+1,j+1} \end{pmatrix} \\ u, v\epsilon\{-1,0,1\} \tag{5}$$

$$C_{i,j}^{Max} = \max(c_{i-1,j-1}, c_{i-1,j}, c_{i-1,j+1}, c_{i,j-1} \\ c_{i,j+1}, c_{i+1,j-1}, c_{i+1,j}, c_{i+1,j+1}) \tag{6}$$

$$\mathrm{ST} = \sqrt{\frac{1}{2}(\mathrm{C}_{\mathrm{i,j}}^{\mathrm{Max}} - \mathrm{C}_{\mathrm{average}}^{\mathrm{d}})^2} \tag{7}$$

$C_{i,j}^{Max}$ demonstrates maximum intensity in neighborhood cells within a selected window around central pixel ($C_{i,j}$). Then, the ratio of ST and $C_{average}^{d}$ are used, which specifies the coefficient of variation between the maximum and average of values neighborhood cells in a selected window around central pixel as (8). Eq. (8) shows the existence of a noisy pixel in (i,j) coordination in Moore neighborhood structure. ε is the constant value in (0.1,0.001) interval. ω is the threshold value for noisy pixel existence which obtains as (9) , (10) and (11).

$$C_{i,j} = \begin{cases} C_{i,j} \text{ is a corrupted pixel} \\ F(i,j) = \dfrac{ST}{C_{average}^{d} + \varepsilon} \le \omega \\ C'_{i,j} \text{is not a corrupted pixel} \\ F(i,j) = \dfrac{ST}{C_{average}^{d} + \varepsilon} > \omega \end{cases} \tag{8}$$

$$C_{Average}^{T} = \frac{1}{N}\sum \begin{pmatrix} (C_{i-1,j-1}, C_{i-1,j}.C_{i-1,j+1}, C_{i,j-1} \\ C_{i,j+1}, C_{i+1,j-1}, C_{i+1,j}, C_{i+1,j+1}) \end{pmatrix} \tag{9}$$

$$ST^{T} = \sqrt{\frac{1}{2}(\mathrm{C}_{\mathrm{i,j}}^{\mathrm{MaxT}} - C_{Average}^{T})^2} \tag{10}$$

$$\omega = \frac{ST^T}{C_{Average}^T + \varepsilon} \tag{11}$$

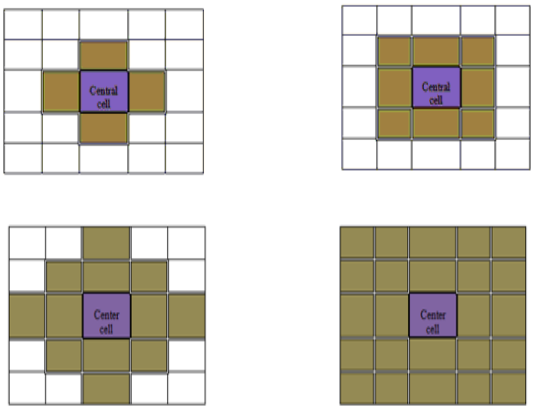

Fig. 1. CA Neighborhood model for Von Neumann (left) and Moore (right) neighborhood of r=1 and r=2. The nearest neighborhood comprises the center cell.

$c_{i-1,j-1}$	$c_{i-1,j}$	$c_{i-1,j+1}$
$c_{i,j-1}$	$c_{i,j}$	$c_{i,j+1}$
$c_{i+1,j-1}$	$c_{i+1,j}$	$c_{i+1,j+1}$

Fig. 2. Centeral cell position in Moore neighborhood model.

Eq.(9) "N" indicates the total number of pixels in selected window (N=8). $C_{i,j}^{MaxT}$ shows maximum intensity within a selected window. At first step, detected pixels may be uncorrupted pixels ($C'_{i,j}$). So, in order to improve accurate rate of noise detection, the first detection pixels are judged again by local fuzzy membership function, which is calculated using equations (12) and (13).

$$C'_{average} = \frac{1}{N}\sum C'_{i+u,j+v} \quad , u,v\epsilon\{-1,0,1\} \tag{12}$$

$$\sigma' = \sqrt{\frac{1}{N}\sum (C'_{i+u,j+v} - C'_{average})^2} \tag{13}$$

Let $C'_{average}$ is average of pixels around uncorrupted pixel ($C'_{i,j}$ center pixel). "N" indicates the total number of pixels in selected window (N=8). σ' is standard deviation of the pixels in selected window. The fuzzy membership degree $\mu_i(c'_{i,j})$ of the center pixel $c'_{i,j}$ in the block is defined as equation (14).

$$\mu_i(c'_{i,j}) = e^{\left(-\frac{(c'_{i,j}-C'_{average})^2}{2\sigma'^2}\right)} \tag{14}$$

The noise candidates are judged again based on the local fuzzy membership function using following equation (15).

$$c'_{i,j} = \begin{cases} c'_{i,j} \text{ is a corrupted pixel} \\ \text{F}(\mu(c'_{i,j})) > \alpha \\ c'_{i,j} \text{ is not a corrupted pixel } = C''_{i,j} \\ \text{F}(\mu(c'_{i,j})) \leq \alpha \end{cases} \tag{15}$$

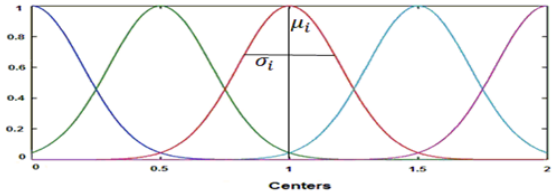

Fig. 3. Gaussian membership function (where μ_i and σ_i are the center and width of the i^{th} fuzzy set Ai, respectively).

$c'_{i,j}$ demonstrates the existence of noise in i,j coordination. $\mu(c'_{i,j})$ is the fuzzy membership degree of the center pixel $c'_{i,j}$ in the selected window. α is the threshold value for noise existence which obtains with using equations (16) , (17) and (18).

$$\alpha=(1\text{-}L_{i,j})\delta \qquad L_{i,j}=\frac{N}{N*N} \tag{16}$$

$$C_{Average}^{T1} = \frac{1}{N-1}\sum \begin{matrix}(C_{i-1,j-1}, C_{i-1,j+1}, C_{i,j-1}, C_{i,j+1} \\ C_{i+1,j-1}, C_{i+1,j}, C_{i+1,j+1})\end{matrix} \tag{17}$$

$$\sigma = \sqrt{\frac{1}{N-1}\sum_{i,j}^{N}(C_{i+u,j+v} - C_{Average}^{T1})^2} \quad u,v\epsilon\{-1,0,1\} \tag{18}$$

"N" indicates the total number of pixels in selected window (N=9). $C_{Average}^{T1}$ shows demonstrates average value of neighborhood cells within a selected window around central pixel ($C_{i,j}$). Therefore, by assuming a threshold (obtained from the experiments), the noisy points can be approximately detected. In equation (16) φ * φ the total number of pixels in the window is 3 * 3. In equation (18) σ is the standard deviation of the pixels around the central cell in the Moor neighborhood.

B) Second phase (The restoration of the corrupted pixels)

The goal of this phase is restoration of the corrupted pixels which uses a two dimensional fuzzy cellular automata with Moore neighborhood structure. In this phase, the cells state is updated in discrete time steps based on transition function F which depends on the current states of the neighbors. Therefore, after determination of the corrupted pixel at the first phase, the neighborhood pixels values around the corrupted pixel can define a membership degree in relation to noisy set based on Moore neighborhood structure by using selected Gaussian membership function. The advantage of Gaussian membership function (see fig.3) is that it is smooth

and nonzero at all points then it will assign a non-zero value for each pixel in that window. See equations (19), (20) and (21).

In this phase, the cells state is updated in discrete time steps based on transition function F that depends on the current states of the neighbors. Therefore, after determination of the corrupted pixel at the first phase, the neighborhood pixels values around the corrupted pixel can define a membership degree in relation to noisy set based on Moore neighborhood structure by using selected Gaussian membership function. The advantage of Gaussian membership function (see fig.3) is that it is smooth and nonzero at all points then it will assign a non-zero value for each pixel in that window. See equations (19), (20) and (21).

$$M' = \frac{1}{N}\sum C'''_{i+u,j+v} \quad C'''_{i+u,j+v} = C'_{i+u,j+v} \quad u,v\epsilon\{-1,0,1\} \tag{19}$$

$$\sigma'^{2} = \frac{1}{N}\sum (C'''_{i+u,j+v} - M')^2 \quad u,v\epsilon\{-1,0,1\} \tag{20}$$

$$\mu_i(C'''_{i+u,j+v}) = e^{\left(-\frac{(C'''_{i+u,j+v}-M')^2}{2\sigma'^2}\right)} \quad u,v\epsilon\{-1,0,1\} \tag{21}$$

M' and σ'^2 are the average and the square deviation of the pixels in Moore neighborhood of the $C'''_{i+u,j+v}$, respectively. Also, for defuzzifying and replacement value based on the average center of gravity using the following equation:

$$Z_{C_{i+u,j+v}} = \frac{\sum \mu_i(C'''_{i+u,j+v})C'''_{i+u,j+v}}{\mu_i(C'''_{i+u,j+v})} \tag{22}$$

Z is the new value of the pixel and can be used as our local state rule function, F of cellular automaton using equation (23).

$$F(C_{i,j}) = Z_{C_{i+u,j+v}} \equiv \frac{\sum \mu_i(C'''_{i+u,j+v})C'''_{i+u,j+v}}{\mu_i(C'''_{i+u,j+v})} \tag{23}$$

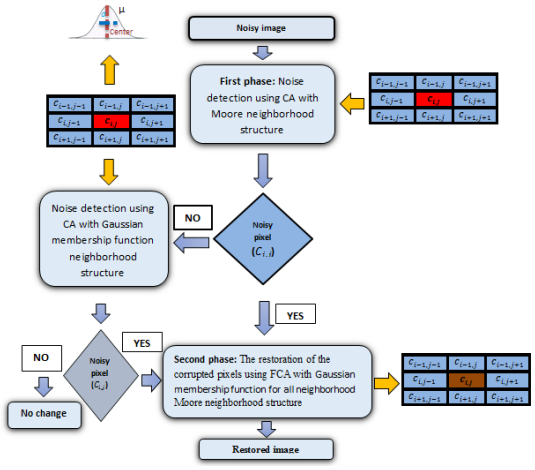

Fig. 4. The flow chart of proposed method.

4. Experimental results

In this section, the proposed method is applied with noise density varied from 10% to 90% with increments of 10% on the 90 test images (see fig.11) such as Lena, Bridge, Peppers and Baboon images by different values of salt and pepper noise. In addition, quantitatively measured performance of the proposed method in comparison with the other methods is evaluated by Peak Signal-to-Noise Ratio (PSNR) which is calculated by Eq (24).

$$PSNR = 10log_{10}\left(\frac{255^2}{MSE}\right) \tag{24}$$

Where 255 is the maximum pixel intensity for 8-bit gray scale images, MSE is the mean square error, which is inserted between the original and restored images, which is calculated by Eq (25):

$$MSE = \frac{1}{m*n}\sum_{i=1}^{m}\sum_{j=1}^{n}(O_{ij} - R_{ij})^2 \tag{25}$$

"O" is the original image (o_{ij} pixel of the original image) and R is the restored image (R_{ij} pixel of the "restored image). In addition, "m" and "n" are the width and height of the image.

The structural similarity (SSIM) index is a method for measuring the similarity between two images and is designed to improve on traditional methods like peak signal-to-noise ratio (PSNR) and mean squared error (MSE), Structural Similarity (SSIM) index is calculated by Eq (26).

$$SSIM = \frac{(2\mu_O\mu_R + c_1)(2\sigma_{OR} + c_2)}{(\mu_O^2 + \mu_R^2 + c_1)(\sigma_O^2 + \sigma_R^2 + c_2)} \tag{26}$$

Where, $\sigma_O = \sqrt{\frac{1}{n-1}\sum_{i=1}^{n}(O_i - \mu_O)^2}$ and $\mu_O = \frac{1}{n}\sum_{i=1}^{n} O_i$ are the variance and average of original image, $\sigma_R = \sqrt{\frac{1}{n-1}\sum_{i=1}^{n}(R_i - \mu_R)^2}$ and $\mu_R = \frac{1}{n}\sum_{i=1}^{n} R_i$ are the variance and average of restored image. $\sigma_{OR} = \sqrt{\frac{1}{n-1}\sum_{i=1}^{n}(O_i - \mu_O)(R_i - \mu_R)}$ is the covariance of original and restored image. L is the dynamic range of the pixel values that for an 8-bit grayscale image composed of 0-255 gray-levels, $c_1 = (k_1L)^2$ and $c_2 = (k_2L)^2$, where $k_1 \ll 1$ and $k_2 \ll 1$ are small constants [27].

Table.1.
Different CA rules performance on images corrupted 70% noise.

Rules	*Baboon PSNR*	*Peppers PSNR*	*Lena PSNR*
Rule 508	23.7	22.7	31.6
Rule 305	22.18	21.18	28.93
Rule 164	18.98	20.98	27.81
Rule 74	16.01	20.01	24.02
Rule 271	20.19	22.28	25.19

Table.2.
Comparison of various filtering techniques and proposed filter base on PSNR values of different noise density for the Lena 512*512 pixel images (Rule 508).

Method	*Noise Ratio%*							
	10	*20*	*30*	*40*	*50*	*60*	*70*	*80*
PSMF	31.1	29.2	27.2	24.1	20.4	15.8	11.3	8.7
TSMF	24.1	26.8	20.6	16.9	13.8	11.1	9.0	7.8
SWMF	33.6	29.3	24.2	19.5	16.3	13.6	11.1	9.3
H.Deng	39.7	37.7	36.5	34.7	33.2	31.8	30.2	28.1
IFCF	32.8	29.3	25.1	21.5	18.4	15.8	13.9	11.9
NSDD	37.4	33.5	30.1	27.7	25.4	24.1	21.4	19.1
FMF	36.4	30.1	23.8	18.7	15.4	12.5	10.6	8.7
ACWMF	30.8	29.3	27.4	22.5	18.7	14.3	11.1	8.5
A.Selmani	40.2	37.6	36.7	34.8	33.1	31.9	30.7	28.9
FRINR	30.3	27.4	25.3	22.7	20.7	19.1	17.1	13.4
IRF	30.6	27.4	22.8	18.3	15.1	12.4	9.9	8.3
Proposed	40.1	37.8	36.9	34.7	33.7	32.4	31.6	29.2

Table.3.
Comparison of various filtering techniques and proposed filter base on PSNR values of different noise density for the Baboon 512*512 pixel images (Rule 508).

Method	*Noise Ratio%*							
	10	*20*	*30*	*40*	*50*	*60*	*70*	*80*
PSMF	28.1	26.7	25.4	23.2	19.8	15.9	11.3	8.7
TSMF	25.2	22.8	19.2	15.9	13.2	10.8	8.9	7.4
SWMF	29.5	26.1	22.3	19.1	15.7	12.9	10.7	8.7
H.Deng	34.8	32.3	29.6	27.9	26.2	24.4	23.0	21.7
IFCF	23.3	22.2	20.4	18.2	15.9	14.3	12.9	12.1
NSDD	31.4	28.3	26.5	24.4	21.1	20.3	18.4	17.1
FMF	27.1	24.4	20.8	18.1	15.4	12.9	11.4	9.8
ACWMF	26.2	24.1	20.5	18.4	16.3	14.5	13.7	10.8
A.Selmani	34.9	32.2	29.5	28.1	26.4	24.5	23.1	21.8
FRINR	26.3	24.8	21.3	19.8	18.5	17.2	15.1	13.8
IRF	25.9	24.3	21.4	17.9	14.8	12.6	10.2	8.4
Proposed	35.1	32.4	29.4	28.3	26.3	24.9	23.7	22.6

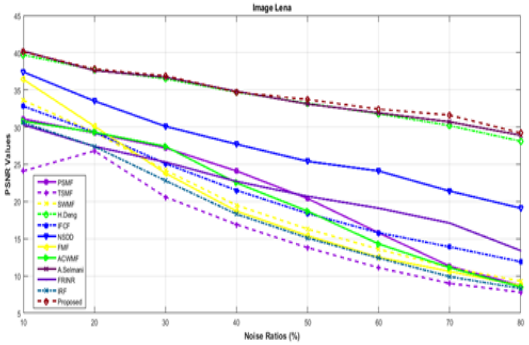

Fig. 5. PSNR values of different filtering techniques at different noise densities for restored Lena image.

Table.4.
Comparison of various filtering techniques and proposed filter base on PSNR values of different noise density for the Peppers 512*512 pixel images (Rule 508).

Method	*Noise Ratio%*							
	10	*20*	*30*	*40*	*50*	*60*	*70*	*80*
PSMF	31.3	28.7	26.3	23.8	19.7	15.8	12.1	10.3
TSMF	30.1	27.3	22.8	18.2	14.5	11.2	10.4	8.1
SWMF	32.5	28.1	23.3	18.4	15.8	12.3	9.8	8.5
H.Deng	33.8	31.4	28.6	26.7	25.1	23.3	21.9	20.6
IFCF	27.2	22.8	19.4	18.3	17.4	15.7	11.9	11.3
NSDD	30.4	27.4	25.5	23.3	20.1	19.3	17.3	16.1
FMF	32.2	29.4	25.5	21.3	17.8	13.5	11.6	10.1
ACWMF	30.7	28.2	23.4	21.8	18.3	15.3	10.7	9.8
A.Selmani	33.9	31.3	28.5	27.2	25.4	23.5	22.1	20.7
FRINR	29.6	25.7	22.5	21.3	19.7	18.5	16.1	14.1
IRF	30.4	25.5	21.8	17.9	14.9	11.8	9.5	7.9
Proposed	34.1	31.5	28.4	27.3	25.3	23.9	22.7	21.6

Table.5.
Comparison of the SSIM values for Lena and Peppers and Baboon 512*512 pixel images, for 70% impulse noise ratio and proposed method (Rule 508).

Methods	*Lena SSIM*	*Peppers SSIM*	*Baboon SSIM*
PSMF	0.52	0.44	0.48
TSMF	0.43	0.32	0.34
SWMF	0.54	0.42	0.49
H.Deng	0.854	0.806	0.829
IFCF	0.67	0.59	0.60
NSDD	0.74	0.63	0.64
FMF	0.51	0.43	0.46
ACWMF	0.53	0.42	0.47
A.Selmani	0.859	0.809	0.831
FRINR	0.72	0.61	0.62
IRF	0.43	0.34	0.36
Proposed	0.863	0.817	0.34

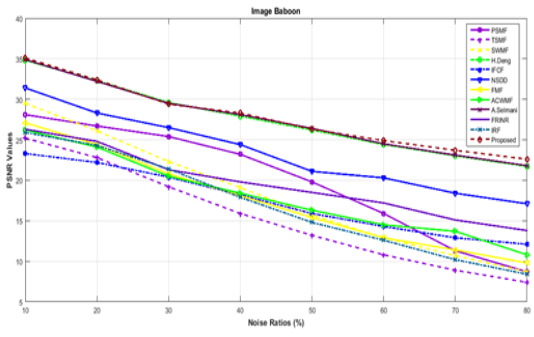

Fig. 6. PSNR values of different filtering techniques at different noise densities for restored Baboon image.

Table.6.
Comparison of various filtering techniques and proposed filter base on PSNR values of different noise density for the Peppers 256*256 pixel images (Rule 305).

Method	***Noise Ratio%***							
	10	***20***	***30***	***40***	***50***	***60***	***70***	***80***
PSMF	29.2	26.6	24.2	21.7	17.6	14.7	11.1	9.3
TSMF	28.0	25.2	20.7	6.1	12.4	10.6	9.4	7.1
SWMF	30.4	26.0	21.2	6.3	13.7	11.2	8.7	7.5
H.Deng	2.5	30.1	29.4	5.9	24.4	22.4	21.1	20.1
IFCF	25.1	20.7	17.3	16.2	15.7	14.6	10.9	10.3
NSDD	29.4	26.1	24.5	22.3	18.9	18.1	16.2	4.8
FMF	30.1	27.3	23.4	19.2	15.7	12.4	10.6	9.1
ACWMF	28.6	26.1	21.3	19.7	16.2	14.2	9.7	8.7
A.Selmani	32.4	30.2	29.5	26.0	24.3	22.5	21.2	20.1
FRINR	27.5	23.6	20.4	19.2	17.6	17.4	15.1	13.1
IRF	28.3	23.4	19.7	15.8	12.8	10.7	8.5	6.8
Proposed	32.3	30.4	29.6	26.1	24.2	22.8	21.8	20.4

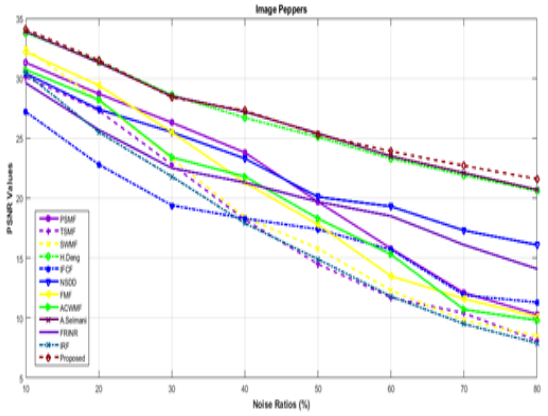

Fig. 7. PSNR values of different filtering techniques at different noise densities for restored Peppers image.

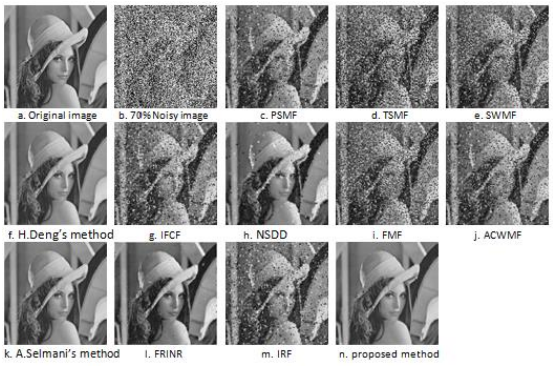

Fig. 8. Restored images of different filters for Lena 512*512 pixel image for 70% impulse noise.

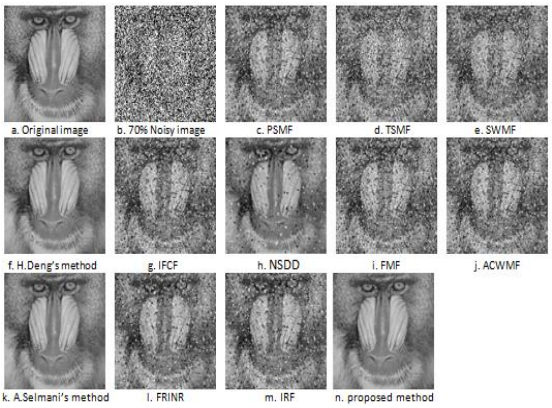

Fig. 9. Restored images of different filters for baboon 512*512 pixel image for 70% impulse noise.

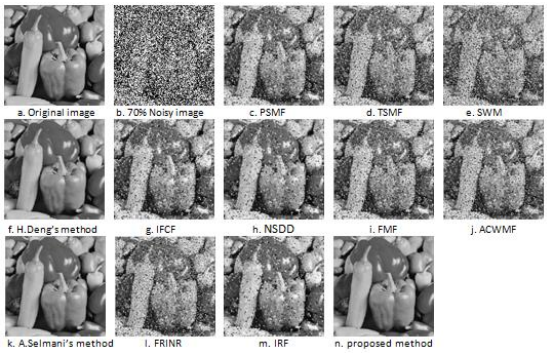

Fig. 10. Restored images of different filters for Peppers 512*512 pixel image for 70% impulse noise.

Fig. 11. Example of 350 test images.

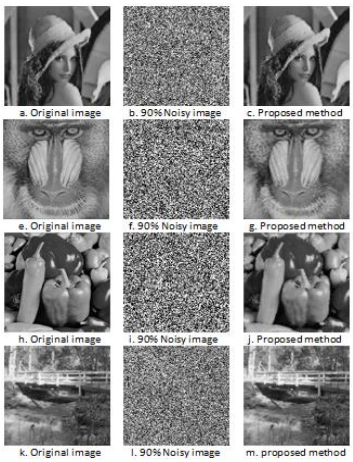

Fig. 12. Restoration images for Lena, Babbon, Peppers and Bridge 512*512 pixel images for 90% impulse noise.

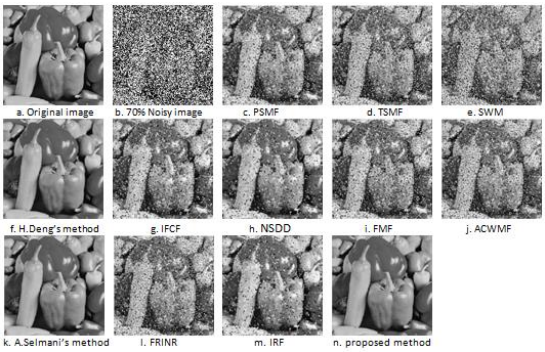

Fig. 13. Restored Peppers image for different algorithms with 256 * 256 pixel images for 70% impulse noise.

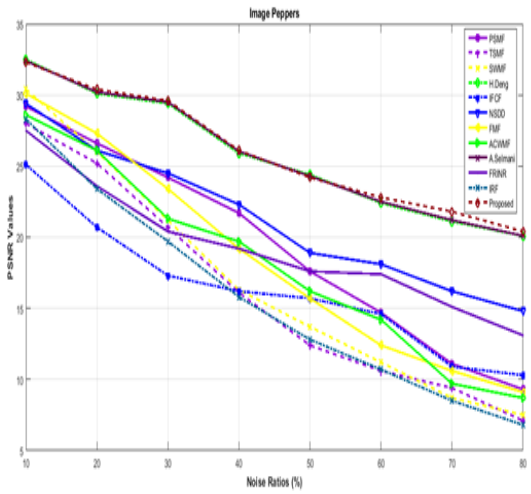

Fig. 14. PSNR values of restored Peppers image for different algorithms with 256 * 256 pixel image.

Restoration performance of RHDINTPM is applying for the several popular test images corrupted by different magnitudes of impulse noise. it is compared with restoration performance of the various filters such as progressive switching median filter (PSMF) [28], tri-state median filter (TSMF) [29], switching median filters (SWMF) [30], H.Deng's method [31], a fuzzy logic control-based approach for image filtering (IFCF) [32], NSDD [33], fuzzy median filter (FMF) [34,35], adaptive impulse detection using center-weighted median filters (ACWMF) [36], A.Selmani's method [37], fuzzy random impulse noise reduction method (FRINR) [38] and impulse rejecting filter (IRF)[39].

Table 1 shows how a cellular automaton works in the proposed method by different types of rules. Table 1, shows that the rule of 508 has better PSNR value than the other rules for Lena, baboon and peppers images. In addition, to reduce computation time, the rule of 305 can be chosen instead of 508 without losing information and image quality.

Tables 2–5 indicates the proposed method performance in terms of the SSIM index and PSNR values. Among the filters, the proposed method produces the highest PSNR values and TSMF produces the lower PSNR values (see tables 2-4). Table 5 shows that the proposed filter gives better SSIM index values for the Lena, Baboon and Peppers images compared to the other filters. Figs. 5-7 shows that the proposed method provides better PSNR curves resulted compared to the other algorithms on ''Lena'', "Baboon" and "Peppers" by different noise intensities ranging from 10% to 90 %, respectively.

Table.7.
Comparison of de-noising time in seconds for the images "Boat" and "Bridge".

Image	*Impulse noise*	*Method*	*Time cost (s)*
Boat	0.2	H. Deng's	124.89
Boat	0.2	NSDD	41.43
Boat	0.2	NFDMF	40.11
Boat	0.2	Proposed method	39.08
Bridge	0.2	H. Deng's method	128.18
Bridge	0.2	NSDD	49.08
Bridge	0.2	NFDMF	45.96
Bridge	0.2	Proposed method	44.81

In addition, figs. 8-10 presents test images corrupted with 70% impulse noise for standard test images that these are showed subjective visual qualities for qualitative analysis of the proposed method and other filtering techniques. TSMF and PSM suppress much of the noise where they fail to preserve edge information while maintaining details of the image. Fig.12 demonstrates subjective quantitative measure as visual by proposed filter with a high noise probability of 90% for "Lena", "Baboon", "Peppers" and "Bridge" standard test images, respectively.

Figures 13 and 14 show the subjective visual qualities and graphical carnations of PSNR for the proposed method. In other sections, it shows other methods for the image of pepper damaged by the noise of 256 x 256 pixels. As shown in Figure 14, the proposed method provides a better PSNR graph compared to other known filtering methods.

Table 6 shows the measure of PSNR for the proposed method and previous methods for the image of peppers with a size of 256 * 256 pixels so that the proposed method shows a better result than the others. At the same images with different sizes, smaller images contain much less information than larger images. Therefore, different values and results are obtained when applying the same images with different sizes or filtering methods. Table 7 shows the processing time of the proposed method for boat and bridge images with a size of 256 * 256 pixels and a density of 0.2 so that the processing

time of the proposed method is faster than the other three methods. Therefore, the proposed method presented in this article to restore images damaged by impulse noise can be implemented with acceptable computation time.

5. Conclusion

In this paper, a novel method for removing impulse noise is presented. The proposed method, RHDINTPM, is based on cellular automata (CA) and fuzzy logic which the statistical features-based filtering technique have been proposed for removing impulse noise from corrupted digital images. The proposed method consists of two phases, which is the special contribution of the new approach to the detection of impulse noise and the restoration of the damaged images. RHDINTPM method is applied to the 90 test images used for evaluation. Numerical measures such as PSNR, SSIM have been computed and values demonstrate that the proposed RHDINTPM method gives better compared to other filtering techniques and can restore meaningful image details at levels of corruption as high as 90%. The main advantage of RHDINTPM is simplicity and parallelism to restore a wide variety of images corrupted by impulse noise. Also, other advantages of the proposed method are the ability to appropriately preserve edges as well as details of the images and robust performance in varying noise intensities ranging from 10% to 90%. Applying other fuzzy filtering methods combined with cellular automata to improve the filtering performance in the presence of different types of high-density noises will be the plan of our future work.

References

[1] Raymond, Chung-Wa, Nikolova, 2005, Salt and pepper noise removal by median-type noise detect or sand detail preserving regularization, IEEE Trans, Image Processing.

[2] Bovik, Handbook of image and video processing, New York: Academic; 2000.

[3] Dharmarajan, Kannan, 2010, A hypergraph-based algorithm for image restoration from salt and pepper noise, Int J Electron Commun (AEU) .

[4] Srinivasan, Ebenezer , 2007, A new fast and efficient decision-based algorithm for removal of high-density impulse noises, IEEE Signal Process Lett.

[5] Yildirim, Basturk, 2008,Yuksel, Impulse noise removal from digital images by a detail-preserving filter based on type-2 fuzzy logic, IEEE Trans Fuzzy Syst.

[6] Bovik, Huang, Munson, 1983, A generalization of median filtering using linear combination of order statistics, IEEE Trans Acoustic Speech Signal Process ASSP.

[7] Huang, Yang, Tang, 1979, Fast two-dimensional median filtering algorithm, IEEE Trans Acoustics Speech Signal Process.

[8] Nodes Jr, Gallagher, 1984, The output distribution of median type filters, IEEE Trans Commun.

[9] Hwang, Haddad, 1995, Adaptive median filters: new algorithms and results, IEEE Trans Image Process.

[10] Ko, Lee, 1991, Center weighted median filters and their applications to image enhancement, IEEE Trans Circuits Syst.

[11] Arce, Paredes, 2000, Recursive weighted median filters admitting negative weights and their optimization, IEEE Trans Signal Process.

[12] Chen, Ma, Chen, 1999, Tri-state median for image de-noising, IEEE Trans Image Process.

[13] Ahmed, Das,2014, Removal of high-density salt-and-pepper noise in images with an iterative adaptive fuzzy filter using alpha-trimmed mean, IEEE512 Trans, Fuzzy Syst.

[14] Zhou, 2012, Cognition and removal of impulse noise with uncertainty, IEEE Trans, Image Process.

[15] Schulte, Witte, Kerre, 2007, A fuzzy noise reduction method for color images, IEEE Trans Image Process.

[16] Toh, Isa, 2010, Cluster-based adaptive fuzzy switching median filter for universal impulse noise reduction, IEEE Trans, Consum. Electron.

[17] Nair, Raju, 2011, Additive noise removal using a novel fuzzy-based filter, Comput Electr Eng .

[18] Tavassoli, Rezvanian, Ebadzadeh, 2010, A new method for impulse noise reduction from digital images based on adaptive neuro-fuzzy system and fuzzy wavelet shrinkage, In: Proceedings of IEEE 2nd 2010 International Conference on Computer Engineering and Technology.

[19] Hussain, Masood Bhatti, Jaffar, 2012, Fuzzy based impulse noise reduction method, Multimedia Tools Appl.

[20] Ulam, 1963, Some Ideas and Prospects in Biomathematics, Annual Review of Biophysics and Bioengineering.

[21] Neumann, 1966, Theory of Self-Reproducing Automata,University of Illinois Press.

[22] Wolfram, 1984, Computation Theory of Cellular Automata, Commun Math Phys .

[23] Selvapeter, Hordijk,2009, Cellular automata for image noise filtering, In: World congress on Nature Biologically Inspired Computing (NaBIC).

[24] Cattaneo, Flocchini, Mauri, Quaranta-Vogliotti, Santoro, 1997, Cellular automata in fuzzy backgrounds, Physica.

[25] Flocchini, Geurts, Mingarelli, and Santoro, 2000, Convergence and aperiodicity in fuzzy cellular automata: revisiting rule 90, Physica D.

[26] Mingarelli, 2006, The global evolution of general fuzzy automata, J. of Cellular Automata.

[27] Sahin, Uguz, Sahin , 2014, Salt and pepper noise filtering with fuzzy-cellular automata, Computers and Electrical Engineering.

[28] Rosin, 2010, Image processing using 3-state cellular automata, Comp Vision Image Unders .

[29] Sadeghi, Rezvanian, Kamrani, 2012, An efficient method for impulse noise reduction from images using fuzzy cellular automata, Int J Electron Commun (AE).

[30] Wang, Bovik, Sheikh, Simoncelli, 2004, Image quality assessment: from error visibility to structural similarity, IEEE Trans Image Process.

[31] Wang, Zhang,1999, Progressive switching median filter for the removal of impulse noise from highly corrupted images, IEEE Trans Circuits Syst II, Analog Digit Signal Process.

[32] Chen, Ma, Chen, 1999, Tri-state median for image denoising, IEEE Trans Image Process .

[33] Zhang, Karim, 2002, A new impulse detector for switching median filters, IEEE Signal Process Lett .

[34] Deng, et, 2017, A decision-based modified total variation diffusion method for impulse noise removal, Hindawi Comput. Intell. Neurosci.

[35] Farbiz, Menhaj,2000, A fuzzy logic control based approach for image filtering, In: E. Kerre, M. Nachtegael, editors. Fuzzy techniques in image processing, 1st ed. Heidelberg, Germany: Physica Verlag.

[36] Wu, Tang, 2011, PDE-based random-valued impulse noise removal based on new class of controlling functions, IEEE Trans. Image Process.

[37] Arakawa, 1999, Median filter based on fuzzy rules and its application to image restoration, Fuzzy Sets Syst .

[38] Arakawa, 2000, Fuzzy rule-based image processing with optimization, In: EE. Kerre, M. Nachtegael, editors, Fuzzy techniques in image processing, 1st ed. Heidelberg, Germany: Physica Verlag.

[39] Chen, Wu, 2001, Adaptive impulse detection using center weighted median filters, IEEE Signal Processing Letters.

[40] Selmani, Seddik, 2018, Anisotropic smart shape-adapted image smoothing without conductance function efficient for impulse noise removal, Digital Signal Processing.

[41] Schulte, De Witte, Nachtegael, der Weken, Kerre,2007, Fuzzy random impulse noise reduction method, Fuzzy Sets Syst.

[42] Chen, Wu, 2001, Adaptive impulse detection using center-weighted median filters, IEEE Signal Process Lett.

[43] Zhang, Han , Dezert , Yi. Yang, 2018, A new adaptive switching median filter for impulse noise reduction with pre-detection based on evidential reasoning, Signal Processing.

[44] Roy, Singha, Shuleenda Devi, Laskar, 2016, Impulse noise removal using SVM classification based fuzzy filter from gray scale images, Signal Processing.

[45] Veerakumar , Narayan Subudhi , Esakkirajan , Kumar Pradhan , 2017, Context model based edge preservation filter for impulse noise removal, Expert Systems With Applications.

[46] Liu, Ni, Ni, 2020, A nonconvex $l_1(l_1 - l_2)$ model for image restoration with impulse noise, Journal of Computational and Applied Mathematics.

[47] Zhang , Han , Yang ,2015, Image segmentation based on evidential Markov random field model, in: IEEE International Conference on Control, Automation and Information Sciences, Changshu, pp.

[48] Wang , Deng ,2016, Modeling object recognition in visual cortex using multi- ple firing k -means and non-negative sparse coding, Signal Process.

[49] Nellro , Thurley , Jonsson , Andersson , 2015,Automated measurement of sintering degree in optical microscopy through image analysis of particle joins, Pattern Recognit.

[50] Turkmen, 2010, Efficient impulse noise detection method with ANFIS for accurate image restoration, Int J Electron Commun (AEU) .